

ARTICLE

<https://doi.org/10.1038/s41467-019-13413-w>

OPEN

LRRK2 kinase activity regulates lysosomal glucocerebrosidase in neurons derived from Parkinson's disease patients

Daniel Ysselstein¹, Maria Nguyen¹, Tiffany J. Young¹, Alex Severino¹, Michael Schwake¹, Kalpana Merchant¹ & Dimitri Krainc^{1*}

Mutations in *LRRK2* and *GBA1* are common genetic risk factors for Parkinson's disease (PD) and major efforts are underway to develop new therapeutics that target LRRK2 or glucocerebrosidase (GCase). Here we describe a mechanistic and therapeutic convergence of LRRK2 and GCase in neurons derived from patients with PD. We find that GCase activity was reduced in dopaminergic (DA) neurons derived from PD patients with *LRRK2* mutations. Inhibition of LRRK2 kinase activity results in increased GCase activity in DA neurons with either *LRRK2* or *GBA1* mutations. This increase is sufficient to partially rescue accumulation of oxidized dopamine and alpha-synuclein in PD patient neurons. We have identified the LRRK2 substrate Rab10 as a key mediator of LRRK2 regulation of GCase activity. Together, these results suggest an important role of mutant LRRK2 as a negative regulator of lysosomal GCase activity.

¹Department of Neurology, Northwestern University Feinberg School of Medicine, 303 E Chicago Avenue, Chicago, IL 60611, USA. *email: dkrainc@nm.org

Parkinson's disease (PD) is the most common neurodegenerative movement disorder that is pathologically characterized with early loss of dopaminergic neurons in the substantia nigra pars compacta (SNc)¹. The identification of a growing number of genetic forms of the disease^{2,3} has provided valuable insights into the cellular pathways that are altered in the disease process and can aid the search for new therapeutic strategies for PD.

Mutations in the gene encoding leucine rich repeat kinase 2 (*LRRK2*) represent one of the most common genetic causes of PD. *LRRK2* is a 286 kDa protein with several functional domains including a kinase domain⁴. To date, over 50 different mutations in the *LRRK2* gene have been reported⁵, with the G2019S point mutation being the most common pathogenic mutation^{5–8}. Pathogenic mutations increase *LRRK2* kinase activity and hence have been classified as gain-of-function mutations^{9,10}. Recently, increased *LRRK2* kinase activity was observed in idiopathic PD and in neurons exposed to mitochondrial toxins, highlighting the possibility of a broader role of *LRRK2* kinase activity in PD pathogenesis¹¹. Despite the significance of *LRRK2* in PD, its physiologic function or pathogenic mechanism underlying PD is not fully elucidated. Increasing evidence suggests a role for *LRRK2* in synaptic function¹² and endo-lysosomal trafficking¹³, although *LRRK2* has also been implicated in cellular proliferation¹⁴, inflammation¹⁵, and cytoskeleton dynamics¹⁶. Unfortunately, the uncertainty in the precise role of *LRRK2* is not resolved by *LRRK2* transgenic or knock-in mouse models due to the lack of a common and consistent phenotype across mouse lines and the inability to recapitulate degeneration of nigral dopaminergic (DA) neurons or synuclein pathology observed in patients with PD^{17,18}. We have recently shown that human DA neurons differentiated from induced pluripotent stem cells (iPSCs) exhibit pathological phenotypes such as accumulation of oxidized dopamine products and neuromelanin that are also observed in PD autopsied brain tissue but not seen in mouse models¹⁹.

The most common risk factor for PD is mutations in the gene *GBA1*, which encodes for glucocerebrosidase 1 (GCase). GCase is a lysosomal hydrolase that catalyzes the hydrolysis of glucosylceramide to glucose and ceramide. Homozygous mutations in GCase that lead to a loss of function result in a lysosomal storage disorder called Gaucher's disease. Heterozygous point mutations represent a major genetic risk factor for PD²⁰ with 7–10% of PD patients harboring a mutation in *GBA1*²¹. Additionally, a growing number of patients have been reported to have concurrent *LRRK2* G2019S mutation with either *GBA1* L444P²² or E326K mutations²³. These patients developed PD symptoms at an earlier age compared to carriers of only *LRRK2* or *GBA1* mutations^{22–24}. Based on these observations, we hypothesized that *GBA1* and *LRRK2* mutations may contribute to PD pathogenesis through a common biological pathway.

To test this hypothesis, we examined GCase activity in DA neurons derived from PD patients and found that *LRRK2* mutations result in reduced lysosomal GCase activity. Inhibition of *LRRK2* kinase activity significantly restored GCase activity in neurons that carry mutations in *LRRK2* or *GBA1*, leading to rescue of PD-associated phenotypes. Our results highlight the potential for *LRRK2* inhibition in idiopathic and *GBA1*-PD and for GCase activation in *LRRK2* patients. These findings could have significant therapeutic implications for these patient populations as therapeutic compounds targeting either *LRRK2* or GCase are currently in clinical trials.

Results

GCase activity is reduced in DA neurons with *LRRK2* mutations. Since patients that carry concurrent *LRRK2* and *GBA1*

mutations develop PD symptoms at an earlier age compared to carriers of single mutations, we first examined the potential role of GCase in *LRRK2*-mediated disease pathogenesis. To this end, fibroblasts were obtained from PD patients carrying *LRRK2* G2019S, R1441C, and R1441G mutations along with healthy controls. Fibroblasts were reprogrammed to iPSCs and then differentiated into dopaminergic neurons²⁵ that were maintained in long-term cultures and analyzed at day 90 post differentiation. We have previously found that these neurons faithfully recapitulate PD disease phenotypes^{19,26}. Lysosomal GCase activity in live cells was measured using the fluorescent quenched substrate PFB-FDGLu that enables real-time analysis of lysosome-specific GCase activity²⁷, unlike traditional approaches which measure activity in lysed cells. Using this approach, we examined the effects of *LRRK2* G2019S mutations on GCase activity in mutant versus control DA neurons and observed a significant reduction in GCase activity in two independent *LRRK2* G2019S iPSC neuronal lines relative to two distinct healthy controls (Fig. 1a). To examine whether this effect was specific to the G2019S mutation, we examined GCase activity in neurons containing *LRRK2* R1441G and R1441C mutations. These mutations also displayed a significant reduction in GCase activity relative to healthy controls (Fig. 1b). In order to generate additional relevant controls, we used CRISPR/Cas9 to correct the point mutations in *LRRK2* G2019S and R1441C iPSCs (Fig. 1c, d). Neurons differentiated from these isogenic lines displayed very similar *LRRK2* expression levels (Supplementary Fig. 3b) and showed a significant recovery in GCase activity for both G2019S (Fig. 1c, e) and R1441C mutations (Fig. 1d, f). Collectively, these results indicate that lysosomal GCase activity is reduced in human DA neurons derived from iPSCs with *LRRK2* mutations.

Inhibition of *LRRK2* increases GCase activity in DA neurons.

Both G2019S and R1441C mutations increase the kinase activity of *LRRK2*^{9,10}. To examine whether the kinase function plays a role in modulating GCase activity in *LRRK2* mutant DA neurons, we treated *LRRK2* G2019S neurons with a potent and well-characterized *LRRK2* kinase inhibitor, MLI-2²⁸. Interestingly, MLI-2 treatment increased GCase activity in two separate DA neuronal cell lines with each *LRRK2* mutation (Fig. 2a). We compared the efficacy of MLI-2 with a modulator of GCase, 6166, developed in our lab²⁹, as well as the mutation corrected *LRRK2* G2019S and R1441C isogenic control lines. Inhibition of *LRRK2* kinase function restored GCase activity to levels observed in respective isogenic control neurons, as well as to levels induced by the GCase modulator (Fig. 2b, c). Next, we tested the specificity of *LRRK2* kinase inhibition effects on GCase activity in DA neurons by testing the effects of MLI-2 on neurons with wild-type (WT) *LRRK2* or mutant GCase. Surprisingly, treatment of healthy control DA neurons with the *LRRK2* inhibitor also led to a significant increase in GCase activity in these cells (Fig. 2d). We then examined the effect of *LRRK2* kinase inhibition on neurons carrying common heterozygous mutations in the *GBA1* gene, E326K or N370S³⁰. To evaluate the significance of any effect on GCase activity, isogenic control lines for *GBA1* E326K and N370S were generated (Supplementary Fig. 1c, d) and simultaneously differentiated into DA neurons (Supplementary Fig. 2c, d). As expected, correction of *GBA1* E326K and N370S mutations significantly increased GCase activity by 54% and 68% respectively (Fig. 2e, f). Interestingly, treatment of these *GBA1* mutant DA neurons with MLI-2 increased GCase activity to levels comparable to those observed in isogenic control neurons (Fig. 2e, f). A similar level of increase was induced by the GCase modulator, 6166 (Fig. 2e, f). Importantly, *LRRK2* expression level was unchanged in these neurons (Supplementary Fig. 3b). Together, these results

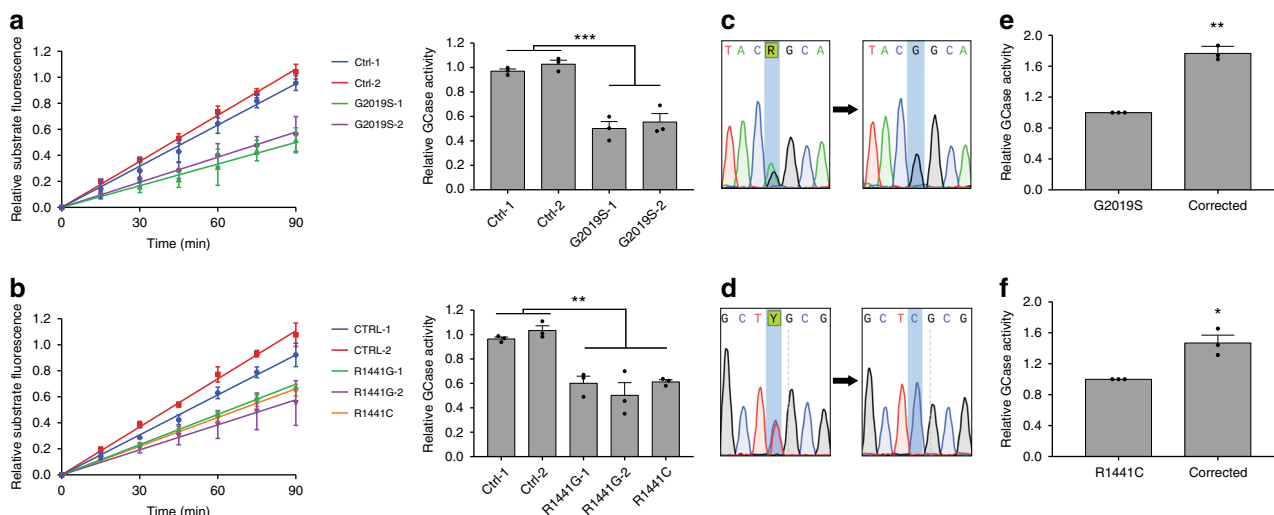


Fig. 1 GCase activity is reduced in DA neurons with *LRRK2* mutations. Live-cell measurement of fluorescent unquenching resulting from hydrolysis of the artificial GCase substrate PFB-FDGl_u by lysosomal GCase in *LRRK2* G2019S (**a** left panel) and R1441G/C (**b** left panel) DA neurons relative to healthy controls over 90 min. GCase activity was determined by analyzing the relative slope of these measurements (**a**, **b** right panel). Sanger sequencing results from *LRRK2* G2019S **c** and R1441C **d** lines and subsequent isogenic controls generated using CRISPR/Cas9. Relative lysosomal GCase activity in DA neurons with *LRRK2* G2019S **e** and R1441C **f** mutations compared to isogenic corrected controls. The data are presented as the mean ± SEM, $n = 3$; $p < 0.05$, $^{**}p < 0.01$, $^{***}p < 0.001$, using one-way ANOVA followed by Tukey's multiple comparison *post hoc* test **a**, **b**, or paired two-tailed *t*-test **e**, **f**. Source data are provided as a Source Data file.

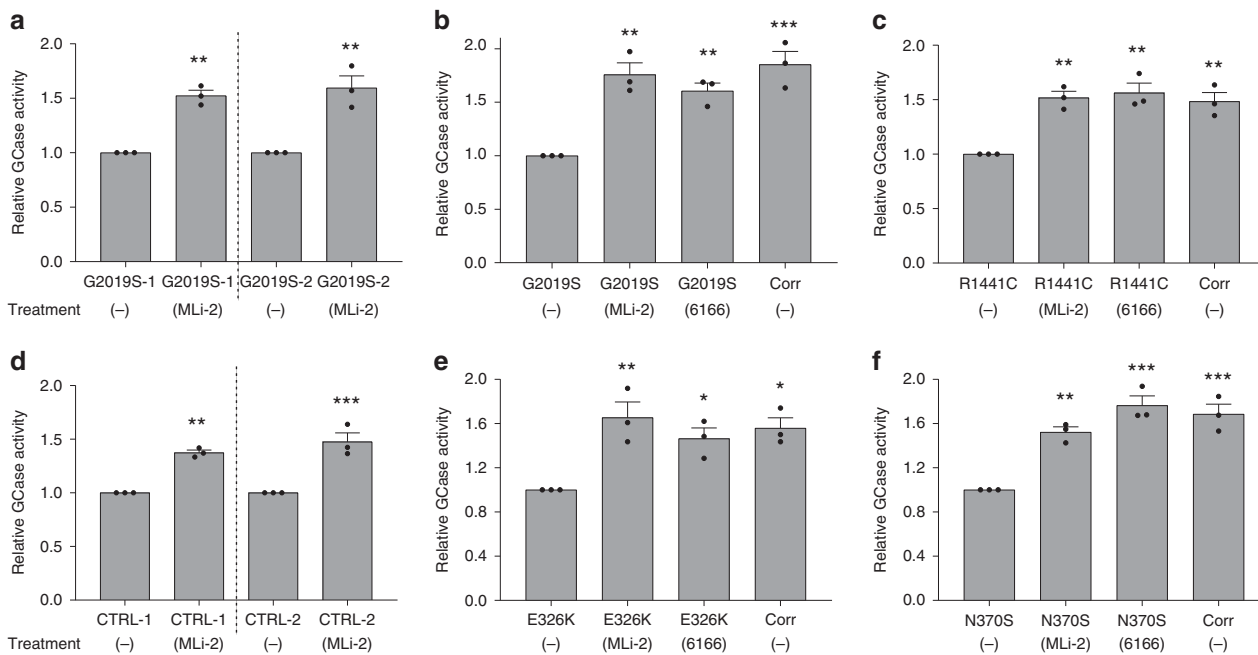


Fig. 2 Inhibition of *LRRK2* kinase activity increases GCase activity in DA neurons from PD patients. Examination of lysosomal GCase activity in *LRRK2* G2019S DA neurons treated with the *LRRK2* kinase inhibitor, MLI-2 (600 nM) **a**. Comparison of GCase activity in *LRRK2* G2019S **b** and R1441C **c** DA neurons relative to isogenic controls and neurons treated with MLI-2 or a direct GCase modulating compound, 6166 (3 μ M). GCase activity measured in DA neurons from two independent healthy controls treated with MLI-2 **d**. Comparison of GCase activity in *GBA1* E326K **e** or N370S **f** DA neurons relative to isogenic controls and neurons treated with MLI-2 or 6166. The data are presented as the mean ± SEM, $n = 3$; $p < 0.05$, $^{**}p < 0.01$, $^{***}p < 0.001$ relative to untreated, one-way ANOVA followed by Tukey's multiple comparison *post hoc* test. Source data are provided as a Source Data file.

highlight an important role of *LRRK2* in regulation of GCase activity in human DA neurons, independent of mutation status or disease state.

LRRK2 inhibition rescues PD-related phenotypes in DA neurons. We have previously shown that iPSC-derived DA neurons

from PD patients accumulate two pathophysiologic markers; dopamine oxidation products¹⁹ and phospho-Ser129-alpha synuclein. Interestingly, treatment with a GCase modulator was found to mitigate both phenotypes. To test whether inhibition of *LRRK2* kinase activity could also reduce these pathophysiologic markers, we compared the effects of MLI-2 and 6166 in DA neurons from patients with *LRRK2* or *GBA1* mutations. When

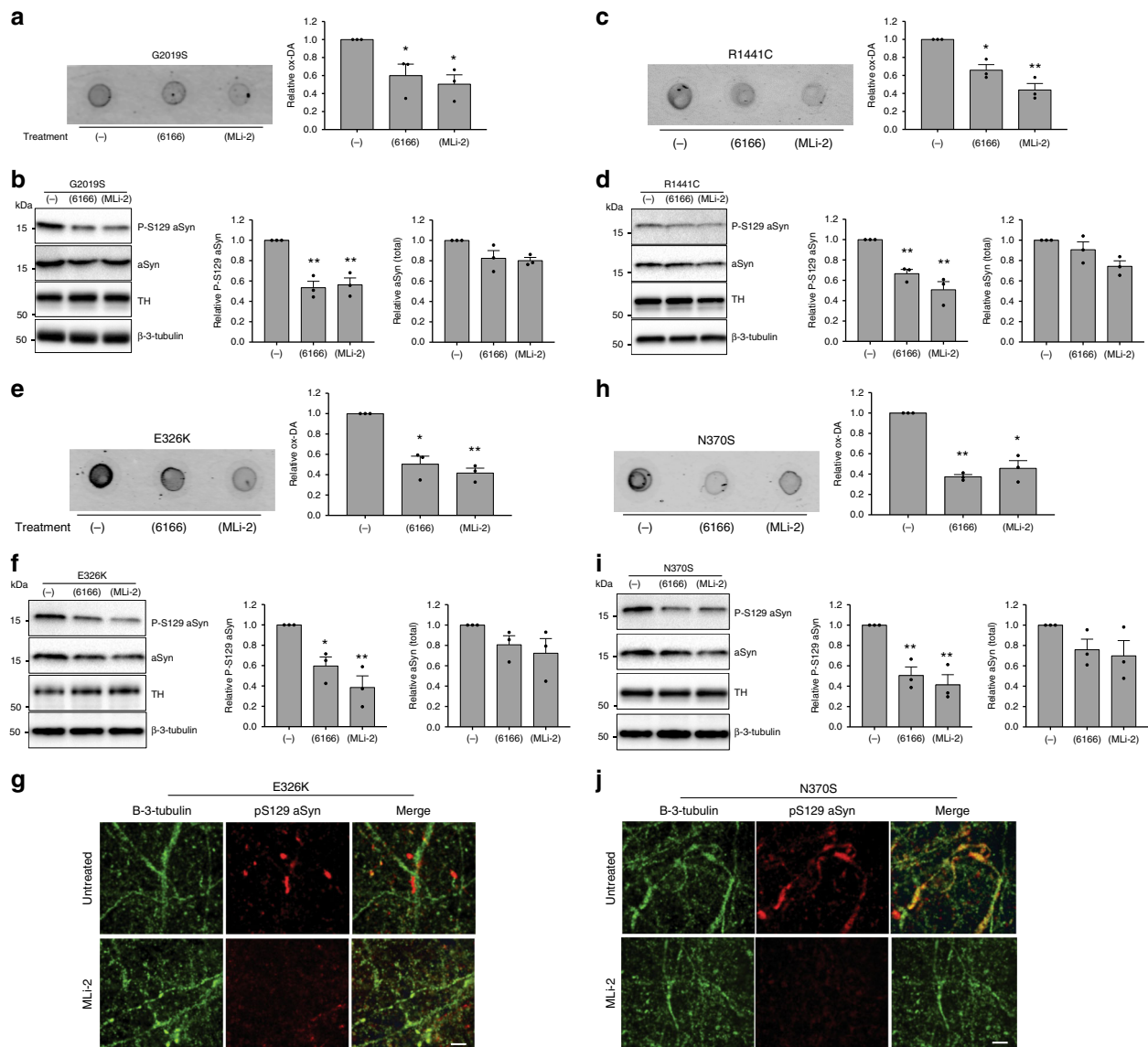


Fig. 3 LRRK2 kinase inhibitors rescue PD-related pathophysiologic phenotypes in LRRK2 and GBA1 mutant neurons. Measurement of insoluble oxidized dopamine by near-IR fluorescence from LRRK2 G2019S **a** and R1441C **c** mutant DA neurons treated with 6166 or MLI-2. Treated cultures were also subjected to western blot analysis of phospho-S129 aSyn (P-S129), total aSyn, and tyrosine hydrolase (TH) with β -3-tubulin used as a loading control **b**, **d**. Measurement of relative levels of insoluble oxidized dopamine by near-IR fluorescence from DA neurons containing GBA1 E326K **e** or N370S **h** mutations. Treated cultures were also subjected to western blot analysis of P-S129, total aSyn, and TH with β -3-tubulin used as a loading control **f**, **i**. Representative images from additional DA neurons containing GBA1 E326K **g** or N370S **j** mutants treated with MLI-2 and stained with antibodies targeted to P-S129 and β -3-tubulin, scale bars, 50 μ m. The data are presented as the mean \pm SEM, $n = 3$; * $p < 0.05$, ** $p < 0.01$ relative to untreated, one-way ANOVA followed by Tukey's multiple comparison *post hoc* test. Source data are provided as a Source Data file.

compared to vehicle-treated DA neurons, MLI-2 or 6166 treatment significantly reduced accumulation of dopamine oxidation products (Fig. 3a, c), as well as phospho-Ser129 alpha synuclein (Fig. 3b, d) in DA neurons with a LRRK2 G2019S or R1441C mutation. Moreover, neurons that carry a GBA1 E326K or N370S mutation also showed a significant reduction in accumulation of dopamine oxidation and phospho-S129 alpha synuclein measured by western blot and immunocytochemistry in response to MLI-2 and 6166 (Fig. 3e–j). Together, these results indicate that LRRK2 kinase inhibitors or GCase modulators have the potential to protect DA neurons with LRRK2 or GBA1 mutations.

GCase activity is negatively regulated by LRRK2 activity. The results described above reveal that LRRK2 kinase activity

negatively regulates GCase activity in DA neurons. To examine whether the effect of LRRK2 on GCase activity is specific to DA neurons we examined GCase activity in fibroblasts from PD patients with and without LRRK2 mutations. As a reference, we also measured GCase activity in fibroblasts from individuals with the GBA1 N370S mutation. Surprisingly, we observed a small (20%), but statistically significant reduction in GCase activity in three separate lines with G2019S mutation relative to WT controls (Fig. 4a). This reduction was not as dramatic as the effect of the GBA1 N370S mutation (Fig. 4b). However, the data indicate that the effect of LRRK2 mutations on GCase activity is not specific to iPSC-derived DA neurons. To determine the role of LRRK2 kinase function in the regulation of GCase activity in the fibroblasts, we examined the effect of two distinct LRRK2 kinase inhibitors, MLI-2 and LRRK2-IN-1. Both LRRK2 kinase

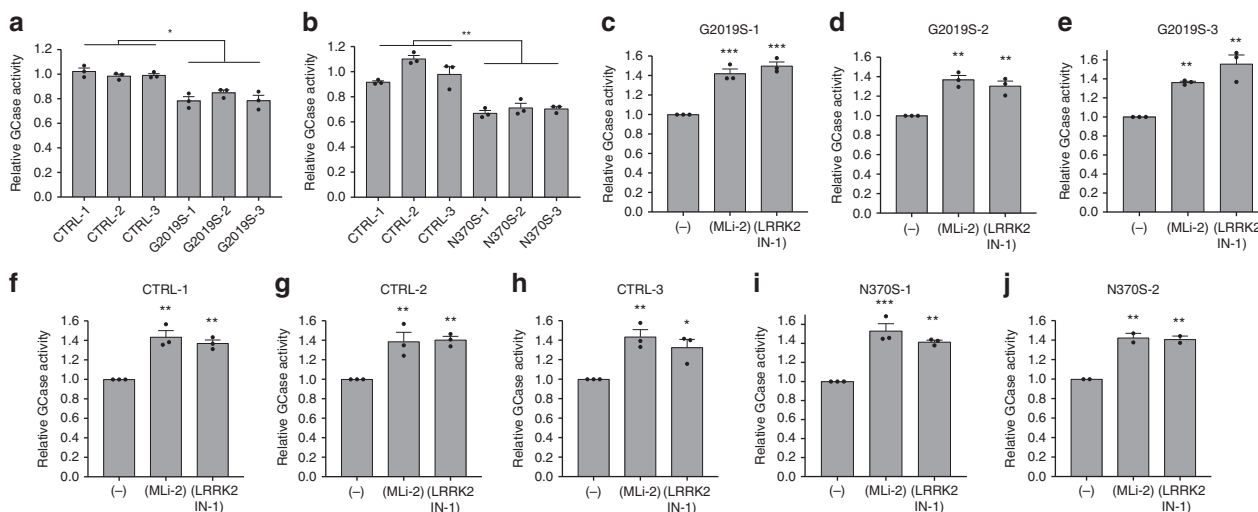


Fig. 4 GCase activity is negatively regulated by LRRK2 kinase activity in patient-derived fibroblasts. Comparison of live-cell lysosomal GCase activity in fibroblasts derived from healthy control individuals, as well as patients with *LRRK2* G2019S **a** and *GBA1* N370S **b** mutations. GCase activity in patient-derived fibroblasts with *LRRK2* G2019S mutations treated with either the LRRK2 inhibitors MLI-2 (600 nM) or LRRK2-IN-1 (2 μ M) **c-e**. GCase activity measured in additional cultures derived from healthy controls **f-h** and from individuals with *GBA1* N370S mutations **i, j** treated with either MLI-2 or LRRK2-IN-1. The data are presented as the mean \pm SEM, $n = 3$ ($n = 2$ for N370S-2); * $p < 0.05$, ** $p < 0.01$, *** $p < 0.001$ relative to healthy controls **a, b** or untreated **c-j**, with one-way ANOVA followed by Tukey's multiple comparison *post hoc* test. Source data are provided as a Source Data file.

inhibitors consistently increased lysosomal GCase activity in the fibroblasts from PD patients with *LRRK2* G2019S mutation (Fig. 4c-e), healthy controls (Fig. 4f-h) or PD patients with *GBA1* N370S mutation (Fig. 4i, j). These results suggest that LRRK2-mediated decrease of GCase activity may involve mechanisms that are not only specific to DA neurons.

LRRK2 regulation of GCase activity is mediated by Rab10.

Recent phosphoproteomics analysis of LRRK2 kinase function has identified a subset of Rab GTPases as substrates of LRRK2 kinase activity³¹. In particular, Rab10 and Rab8 were identified as LRRK2 substrates with a potential role in endolysosomal function and lysosomal homeostasis³². For these reasons, we sought to examine whether Rab8 or Rab10 were responsible for the regulation of GCase activity by LRRK2. To this end, lentivirus encoding shRNA targeted to Rab10 and Rab8 were generated. Transduction of Rab10 and Rab8 shRNA in fibroblasts led to a significant reduction in the levels of the respective protein relative to scrambled controls (Fig. 5a). Interestingly, knock down of Rab10, but not Rab8, significantly reduced lysosomal GCase activity in the fibroblasts derived from healthy controls and *LRRK2* G2019S PD donors (Fig. 5b-e). Consistent with the greater kinase activity of LRRK2 G2019S, the basal steady state levels of phospho-Rab10 were $\sim 50\%$ higher in G2019S cells as compared to WT controls (Fig. 5f). Similarly, there was $\sim 40\%$ increase in Rab10 phosphorylation in DA neurons derived from *LRRK2* G2019S or R1441C PD donors compared to their respective isogenic controls (Fig. 5h). Treatment of the fibroblasts with MLI-2 significantly ($\sim 60\%$) reduced the levels of phosphorylated Rab10, consistent with previous reports in a variety of cell types (Fig. 5g). However, we did not observe a reduction in GCase protein, indicating that the regulation of GCase activity by LRRK2 is independent of GCase protein expression. Treatment of DA neurons with MLI-2 also significantly (80%) reduced the levels of phosphorylated Rab10 (Fig. 5i).

To further demonstrate a role of Rab10 in regulation of GCase activity, we used lentiviral transduction to express Rab10 WT or phospho-mimic T72E Rab10 in control fibroblasts and examined GCase activity (Fig. 6a). Overexpression of Rab10 WT, but not

the phospho-mimic, increased GCase activity in the fibroblasts (Fig. 6a-c). Similarly, overexpression of WT Rab10 in DA neurons with LRRK2 R1441C or G2019S mutations (Fig. 6d, e), as well as neurons with *GBA1* N370S or E326K mutations (Fig. 6f, g) resulted in significantly increased GCase activity relative to transduced controls. To confirm that the LRRK2 inhibitors are working directly through LRRK2, we first examined phosphorylation of serine 935, which can be used as a proxy measure of LRRK2 kinase activity³³. We found that LRRK2 and *GBA1* mutant neurons treated with MLI-2 display a reduction in phospho-S935 (Supplementary Fig. 3c, d). Additionally, we employed lentivirus encoding shRNA targeted to LRRK2 to knock down LRRK2 expression in three control fibroblast lines (Supplementary Fig. 3e) and treated these cells with MLI-2 along with the WT cells transduced with scrambled shRNA controls. Consistent with our previous result (Fig. 4f-h), treatment of WT cells with MLI-2 significantly increased GCase activity, however, treatment of LRRK2 knockdown cells with MLI-2 had no effect on GCase activity (Supplementary Fig. 3g-i). Despite the changes in GCase enzymatic activity, we did not observe a change in GCase protein level as a result of LRRK2 or Rab10 knockdown in these cells (Supplementary Fig. 3c). Surprisingly, knockdown of LRRK2 did not have the same effect on GCase activity as treatment with MLI-2 (Supplementary Fig. 3g-i). Further examination of LRRK2 knock-down cells revealed a significant reduction ($> 60\%$) in Rab10 protein levels relative to control transduced cells (Supplementary Fig. 3f). Loss of Rab10 may explain why GCase activity is not increased as a result of LRRK2 knockdown similar to MLI-2 treatment (Supplementary Fig. 3g-i). Together, these data highlight Rab10 as a key mediator of LRRK2 regulation of GCase activity in human fibroblasts and DA neurons.

Discussion

The recent identification of patients with both *LRRK2* and *GBA1* mutations who exhibit PD symptoms at an earlier age compared to carriers of single *LRRK2* and *GBA1* mutations²²⁻²⁴ led us to examine possible mechanistic convergences of *LRRK2* and *GBA1* in PD pathogenesis. In this study, we have shown that GCase

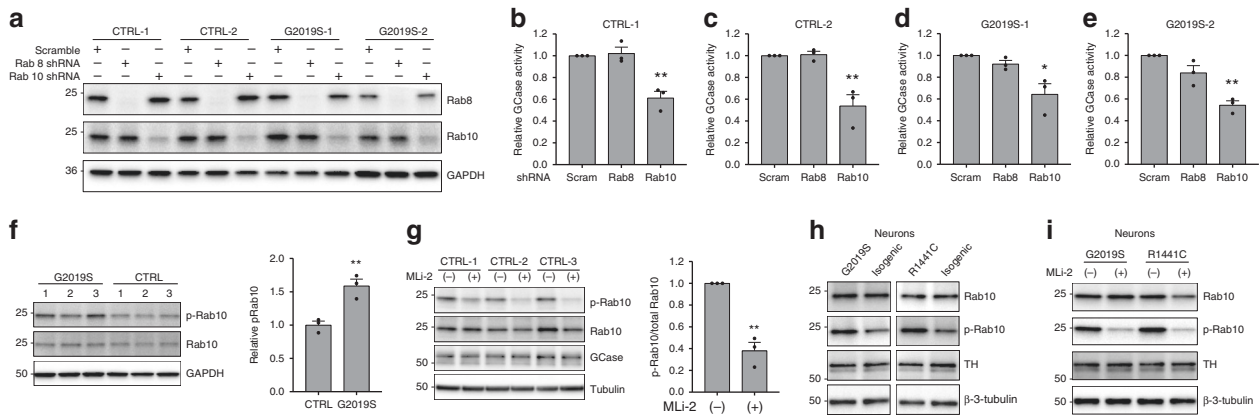


Fig. 5 Rab10 is a mediator of GCase activity by LRRK2 in fibroblasts and DA neurons. Western blot analysis of fibroblasts, from healthy controls or from patients with the *LRRK2* G2019S mutation treated with lentivirus encoding Rab8 and Rab10 shRNA, probed for Rab8, Rab10, and GAPDH (loading control) **a**. Examination of relative lysosomal GCase activity in fibroblasts upon Rab8 and Rab10 knock-down **b-e**. Western blot analysis of fibroblasts from 3 patients with *LRRK2* G2019S and from 3 healthy controls were probed for phospho-Rab10 (p-Rab10), Rab10, and GAPDH (loading control). The data is presented as the average p-Rab10 signal for the 3 G2019S samples relative to the 3 controls **f**. Western blot analysis of fibroblasts from 3 controls treated with MLI-2 were probed for phospho-Rab10 (p-Rab10), Rab10, GCase, and tubulin (loading control). Data is presented as the ratio of p-Rab10 to total Rab10 for the treated relative to untreated cells **g**. Representative western blots of lysates from *LRRK2* G2019S and R1441C DA neurons relative to the corresponding isogenic controls **h** or relative to MLI-2 treated neurons **i** were probed for p-Rab10, Rab10 and β -3-tubulin (loading control). The data are presented as the mean \pm SEM, $n = 3$; * $p < 0.05$, ** $p < 0.01$, using one-way ANOVA followed by Tukey's multiple comparison *post hoc* test **b-e**, or paired two-tailed *t*-test **f, g**. Source data are provided as a Source Data file.

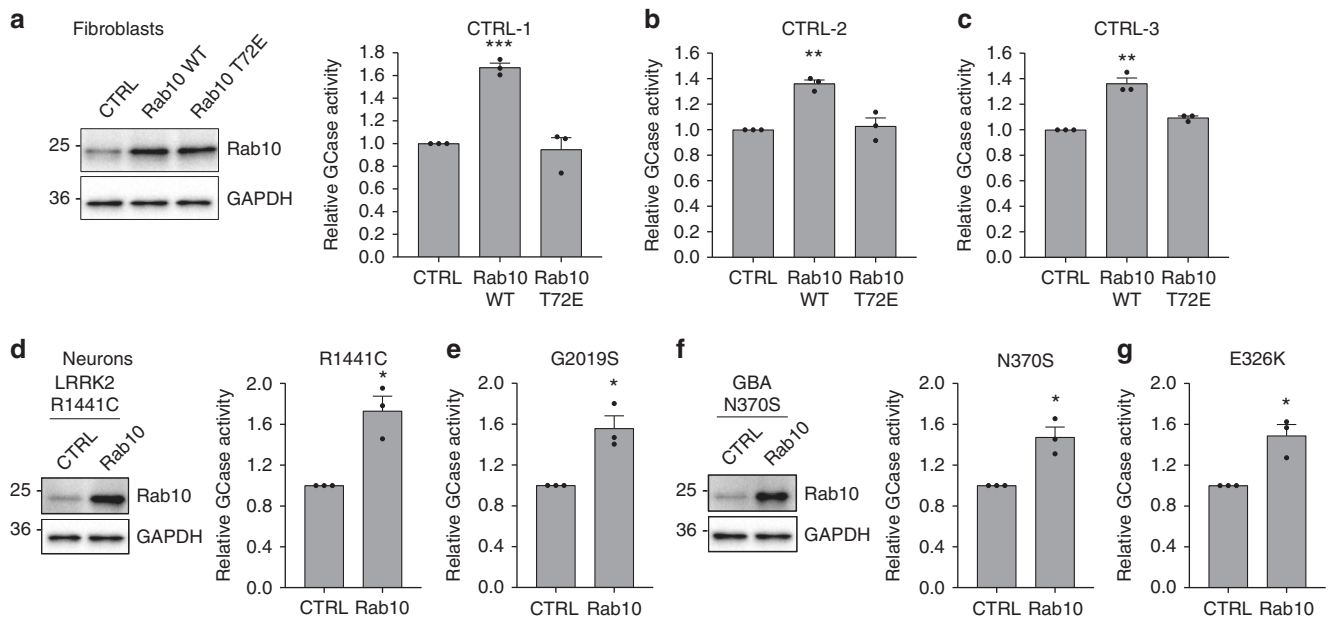


Fig. 6 Overexpression of Rab10 WT increases GCase activity in fibroblasts and DA neurons. Relative GCase activity in control fibroblasts transduced with lentivirus expressing GFP, Rab10 WT or Rab10 T72E **a-c**. Representative western blots showing overexpression of Rab10 and Rab10 T72E in control (CTRL) fibroblasts (**a** right). Relative GCase activity in DA neurons containing *LRRK2* R1441C **d**, *LRRK2* G2019S **e**, *GBA1* N370S **f**, or *GBA1* E326K **g** mutations transduced with CTRL or Rab10 lentivirus for 10 days, with representative western blots showing overexpression of Rab10 in DA neurons (**f** right). The data are presented as the mean \pm SEM, $n = 3$; * $p < 0.05$, ** $p < 0.01$, *** $p < 0.001$, using one-way ANOVA followed by Tukey's multiple comparison *post hoc* test **a-c**, or paired two-tailed *t*-test **d-g**. Source data are provided as a Source Data file.

activity is reduced in human dopaminergic neurons as a result of *LRRK2* mutations. On the other hand, *LRRK2* kinase inhibitors restored GCase activity in neurons that carry mutations in *LRRK2* or *GBA1*, and rescued neurons from PD-associated phenotypes including accumulation of dopamine oxidation products and accumulation of phospho-S129 alpha synuclein. Lastly, we have identified the *LRRK2* substrate, Rab10, as the key mediator of *LRRK2*-mediated regulation of GCase activity.

Mutations in *GBA1*, which lead to a reduction in GCase activity, represent an important risk factor for the development of PD³⁴. Moreover, we have shown previously that accumulation of misfolded alpha synuclein can also lead to reduction of wild-type GCase in the lysosome²⁶, suggesting that the wild-type enzyme activity may be decreased in sporadic forms of PD. This notion was supported by recent studies that found a modest reduction in GCase activity in idiopathic PD patients without

GBA1 mutation^{35,36} highlighting the importance of wild-type GCCase activity in idiopathic PD. In addition, we have previously shown that increased levels of cytosolic oxidative stress can promote oxidation of dopamine which can covalently modify GCCase at critical catalytic cysteine residues leading to reduced enzymatic activity¹⁹. This effect was observed in human DA but not mouse DA neurons highlighting physiological differences in handling of dopamine by human neurons which uniquely accumulate neuromelanin³⁷. Since an increase in dopamine oxidation was also seen in *LRRK2* mutant neurons, we hypothesized that oxidized DA could contribute to the reduction in GCCase activity observed in these neurons^{12,37}. In *LRRK2* mutant neurons, we observe an accumulation of misfolded phospho-S129 alpha synuclein indicating that alpha synuclein accumulation, together with oxidized dopamine, may also play a potential role in reduced GCCase activity in mutant DA neurons.

While these mechanisms may explain the reduction in GCCase activity observed in *LRRK2* mutant neurons, we also observed a modest reduction in lysosomal GCCase activity in patient-derived fibroblasts with *LRRK2* mutations. Since fibroblasts do not produce dopamine and express only a low level of alpha synuclein, we hypothesized that an alternative mechanism must be responsible for reduction of GCCase in these cells. To this end, we identified a direct role of *LRRK2* on regulation of GCCase activity through Rab10 phosphorylation. This was confirmed by both *LRRK2* and Rab10 knock-down, which abolished the effect of treatment with *LRRK2* inhibitor on GCCase activity in these cells. Interestingly, while live-cell lysosomal GCCase activity was significantly increased upon treatment with *LRRK2* kinase inhibitor and reduced upon knock-down of Rab10, we observed no change in total cellular GCCase protein. This suggests that *LRRK2* may regulate the lysosomal environment through Rab10 which is consistent with the recent observation of the role of Rab10 in lysosomal homeostasis³².

In our experiments, increased Rab10 phosphorylation was comparable to Rab10 knock down in reducing GCCase activity, consistent with the recent report that phosphorylation of Rab10 by *LRRK2* leads to deactivation of Rab10 protein function¹¹. Interestingly, while inhibition of *LRRK2* kinase activity significantly increased GCCase activity in patient-derived fibroblasts, knock-down of *LRRK2* had an opposite effect and reduced GCCase activity. This apparently contradictory result could potentially be explained by the significant decrease in Rab10 levels seen in these cells as a result of *LRRK2* knock-down that is not observed upon kinase inhibition. Exactly how *LRRK2* knock-down effects Rab10 protein levels remains of considerable interest and requires additional investigation. The current data suggest that some additional function of *LRRK2*, independent of *LRRK2* kinase activity, is affected by knock-down of the protein. This could be through loss of *LRRK2* GTPase activity³⁸ or loss of *LRRK2* scaffolding function in regulation of signaling cascades³⁹.

Considerable efforts have been focused on development of therapeutic agents to target *LRRK2* and GCCase. *LRRK2* kinase inhibitors are currently in phase 1b clinical trials in PD patients with and without *LRRK2* mutations (NCT03710707). Our results define a mechanism through which *LRRK2* inhibition could be therapeutically beneficial for the treatment of the broader PD population, as well as for *GBA1*-PD patients. In addition, recent observations have described an increase in WT *LRRK2* kinase activity in idiopathic PD¹¹. Intriguingly, based on our results, this increase in *LRRK2* activity in idiopathic PD may also contribute to reduced GCCase activity in the absence of *GBA1* mutations^{35,36}. In addition to *LRRK2* inhibition, activation of GCCase is another strategy that has exciting therapeutic potential³⁴. GCCase activators are also currently in clinical trials for individuals with *GBA1*-PD (NL7061, NL6574). While these trials are currently limited to

patients with *GBA1*-PD, our observation that GCCase is consistently reduced in *LRRK2* mutant neurons suggest that *LRRK2* patients could benefit from GCCase activation. In conclusion, our results highlight the potential for existing therapeutic strategies targeting *LRRK2* and GCCase to have a broader application for PD patients.

Methods

Antibodies. For western blot analysis rabbit anti-rab10 (Cell Signaling, 8127S, 1:1000), rabbit anti-phospho-rab10 (Abcam, ab230261, 1:1000), rabbit anti-rab8 (Cell signaling, 6971S, 1:1000), mouse anti- β -3-tubulin (Cell signaling, 4466S, 1:4000), rabbit anti-TH (Millipore, 657012, 1:4000), rabbit anti pS129 aSyn (Abcam, ab51253, 1:1000), mouse anti alpha synuclein (BD Biosciences, 610787, 1:2000), rabbit anti-*LRRK2* (Abcam, ab133474, 1:500), rabbit anti-phospho S935 *LRRK2* (Abcam, ab133450, 1:500), rabbit anti-alpha synuclein (SantaCruz, SC7011-R, 1:2000), rabbit anti-Glucocerebrosidase (Sigma, G4171), mouse anti-alpha tubulin (Sigma, T5168, 1:40,000), mouse anti-GAPDH (Millipore, MAB374, 1:5000). The secondary antibodies used in western blot analysis goat anti-mouse and goat anti-rabbit (Jackson ImmunoResearch lab, #115-035-146, #111-035-144, 1:10,000). For immunocytochemistry, rabbit anti-pS129 aSyn (Abcam, ab51253, 1:200), mouse anti- β -3-tubulin (BioLegend, 801202, 1:500), rabbit anti- β -3-tubulin (BioLegend, 802001, 1:500), sheep anti-TH (Novus, NB300-110, 1:500) mouse anti-MAP2 (Sigma, M4403, 1:500).

Human iPSC culture and differentiation. All cell lines were obtained from the Northwestern University Biorepository or from the NINDS Human Cell and Data Repository. To ensure that the cell lines did not contain unknown *GBA1* mutations, all exons of *GBA1* were sequenced in the cell lines examined. Additionally, exon 31 and 41 of *LRRK2*, which contain the overwhelming majority of *LRRK2* mutations were also sequenced. Human iPSCs were generated from skin fibroblasts through retroviral expression of OCT4, SOX2, cMyc, KLF4⁴⁰. iPSCs were validated by qPCR analysis comparing expression of classical stem cell markers relative to embryonic stem cells including KLF4, UTF1, DNMT3B, SOX2, cMyc, OCT4, Nanog, and TDGF1 (Supplementary Fig. 1a-d) using established primers (Supplementary Methods). For qPCR, RNA was isolated using RNeasy kit (Qiagen) and transcribed to cDNA using the High-Capacity cDNA Reverse Transcription Kit (ThermoFisher). qPCR was performed in the 7500 Fast Real-Time PCR system (Applied Biosystems), using ssoAdvanced universal SYBR Green Supermix (BioRad). All lines were routinely tested for mycoplasma contamination using PCR based detection (Venor GeM Mycoplasma Detection Kit (Sigma, MP0025)).

iPSCs were continuously maintained in mTeSR1 (StemCell Technologies) with manual passaging once a week prior to differentiation. Dopaminergic neuron differentiation was performed using the Kriks et al. protocol²⁵. Cells were passaged in 1 mm chunks on day 13 to 10 cm dishes coated with poly-D-lysine (PDL)/laminin. At day 25, cells were treated with Accutase to achieve single cell populations and plated onto PDL/laminin coated tissue culture plates. Following this final passage, cells were fed every 3 days with Neurobasal Media (Gibco) + SM1 supplement (Stemcell Technologies) containing BDNF, ascorbic acid, GDNF, TGF- β 3, cAMP, and DAPT until day 40. After day 40, cells were maintained in Neurobasal + SM1 supplement twice weekly. Quality control was performed by immunocytochemistry on each differentiation set to ensure efficient differentiation (β -III-tubulin positive > 99%) with equivalent expression of midbrain specific markers among compared lines (TH > 60%) (Supplementary Fig. 2)¹⁹.

Generation of isogenic lines. Optimal CRISPR guides were chosen using the CRISPOR design tool⁴¹ to target *LRRK2* or *GBA1* mutation. Guides were cloned into pSpCas9(BB)-2A-GFP (pX458, Addgene #48138) and Sanger sequenced to ensure proper cloning. iPSC colonies grown on a 10 cm dish were dissociated using Accutase and 5 million cells were transduced with 3 μ g CRISPR guide, along with 4 μ g ssODN using the Neon transfection system (Thermo Fisher). Transduced cells were then plated using mTeSR with 10 μ M ROCK inhibitor. After 48 h, GFP positive cells were sorted and plated at clonal density (10,000 cells/plate) on Matrigel coated 10 cm dishes. Individual colonies were manually passaged and plated in 48 well plates. Clones were grown to confluence and passaged using Accutase. About 15% of cells were replated and the remaining were used for Sanger sequencing reactions. Crude genomic DNA was obtained using Viagen extraction reagents. Corrected clones were expanded, resequenced, and submitted for g-band karyotype analysis (Cell Line Genetics).

Treatment conditions. Differentiated dopaminergic neurons 80 days in culture were treated every 2 days for 12 days with 600 nM MLI-2 which significantly inhibits *LRRK2*, or 3 μ M 6166 which was found previously to promote robust GCCase modulation²⁹ prior to analysis. Treatments for GCCase activity measurements and biochemical assays were performed simultaneously on neurons derived from identical differentiations. Sample numbers listed in the figure legend represent separate DA neuron differentiations. For assays using fibroblasts, cells were pre-treated for 3 days with 600 nM MLI-2, 2 μ M *LRRK2*-IN-1⁴² and 3 μ M 6166²⁹ prior to analysis.

Live cell GCCase assay. At day 25 after differentiation, dopaminergic neural precursor cells were dissociated and plated on black 96-well plates (40,000 cells/well) coated with poly-D-lysine and laminin. GCCase activity was assessed in culture using the fluorescent quenched substrate 5-(pentafluorobenzoylamino) fluorescein di- β -D-glucopyranoside (PFB-FDGLu) (Thermo Fisher). Following a wash with phenol red free Neurobasal media, 100 μ L of phenol red free Neurobasal + SM1 supplement containing 50 μ g/mL PFB-FDGLu was added to each well. Supplemental wells were also treated with 400 nM bafilomycin A1. Cells were pre-incubated for 60 min at 37 °C to allow for the substrate to accumulate in the lysosome and hydrolysis was monitored using a plate reader to monitor unquenching of the fluorescent probe every 15 min for 90 min at 485/525 nm (excitation/emission). For fibroblasts, substrate was pre-incubated for 75 min and plates were read every 20 min for 120 min. Lysosomal hydrolysis of the substrate was determined by subtracting the signal obtained from bafilomycin A1 treated cells from the total fluorescence intensity. Lysosomal GCCase activity was considered the bafilomycin A1 sensitive fraction of the fluorescent signal. Following the activity measurements, cells were washed in 1 \times PBS, lysed in RIPA buffer, and the total protein concentration was determined using the standard BCA Assay. Lysosomal GCCase activity was then normalized to total protein concentration.

Western blot analysis. To obtain samples for western blot analysis, media was aspirated from neurons plated on 12-well or 6-well plates. Cells were washed in 1 \times PBS, scraped off the plate, pelleted in 1.5 mL microcentrifuge tubes, and stored at -80 °C until further use. The cells were lysed on ice in RIPA buffer (50 mM Tris HCl, pH 7.4, 150 mM NaCl, 0.1% (w/v) SDS, 0.5% (w/v) sodium deoxycholate, 1% Triton X-100) with HaltTM protease/phosphatase inhibitor cocktail (Thermo Scientific). Lysates were cleared by centrifugation at 20,000 \times g, and the protein concentration was determined using a BCA protein assay kit. Lysates were denatured by heating in 4X Laemmli sample buffer (BioRad). Equal amounts of protein were separated using precast, 4–12% or 4–20% Tris-glycine gels. Proteins were transferred onto PVDF membrane using the Transblot Turbo transfer system (BioRad). Blots used to detect alpha-synuclein or Rab proteins were pre-fixed in 0.5% paraformaldehyde for 20 min. Membranes were blocked with 10% milk in TBS-T (50 mM Tris, pH 7.4, 150 mM NaCl, 0.1% Tween20). Membranes were incubated with primary antibody overnight at 4 °C. After washing, membranes were incubated with horseradish peroxidase-conjugated anti-rabbit or anti-mouse secondary antibody for 1.5 h at room temperature. Chemiluminescence was assessed using pico or femto chemiluminescence substrates (Thermo Fisher). Bands were imaged on a ChemiDoc XRS + imaging station with a 16-bit CCD camera. Quantification of protein bands was done using ImageJ software (NIH). Normalization was performed using β -3-tubulin signal in neurons and α -tubulin or GAPDH signal in fibroblasts.

Near infrared fluorescence detection of oxidized dopamine. Accumulation of neuromelanin-like dopamine oxidation products was measured, as previously described¹⁹ with some modification. Briefly, dopaminergic neurons were lysed with RIPA buffer and centrifuged at 20,000 \times g for 20 min. The protein concentration from the resulting supernatant was determined using a BCA Assay. Protein in the resulting insoluble material was extracted by resuspending the pellet in 1 \times PBS with 2% SDS, boiled for 5 min, sonicated, and boiled for an additional 5 min. The samples were then centrifuged at 100,000 \times g for 20 min and the supernatant was removed. The resulting pellet was extracted in 4 N NaOH overnight at 55 °C. The total protein in the lysate was used to determine the volume of 4 N NaOH to add to the insoluble pellet to compensate for differences in starting cell number, ensuring equal loading. In total, 10 μ L was blotted onto Biodyne B nylon membrane (Pall Life Sciences). Membranes were imaged on the Odyssey CLx (LI-COR Biosciences) using the 700 nm excitation wavelength. Spot intensity was analyzed using ImageJ software (NIH).

Immunocytochemistry. Neurons plated on nitric acid-treated coverslips were washed with 1 \times PBS and fixed using 4% paraformaldehyde for 10 min at room temperature. Cells were permeabilized using 0.1% saponin in 1 \times PBS, then blocked in 1 \times PBS, 0.1% saponin, 10% FBS, 1% BSA for 20 min. Fixed cells were incubated with primary antibodies overnight at 4 °C, washed three times in 1 \times PBS, then incubated with secondary antibodies for 1 h at room temperature. Coverslips were mounted onto slides using Vectashield + DAPI (Vector Labs). Images were acquired on the Leica DMI4000B or the Nikon AIR confocal microscopes.

Generation of lentiviral constructs. Rab8, Rab10, and LRRK2 shRNA constructs were obtained from Sigma. Rab10 WT and T72E were cloned into the pER4 lentiviral expression vector using standard cloning techniques. Lentiviral vectors along with helper plasmids, pLP3 (Invitrogen) and psPAX2 (Addgene, #12260), were transfected into HEK-FT cells using X-treme Gene HP DNA Transfection Reagent (Roche). The resulting virus particles were purified and concentrated using LentiX-concentrator (Clontech). Virus titers were determined using the RETROtek p24 Antigen ELISA kit (ZeptoMetric Corporation). Concentrated virus was stored in single use aliquots at -80 °C.

Statistical analysis. Statistical calculations were performed using GraphPad Prism 7 software. Datasets with two samples were analyzed using a two-tailed *t*-test. Datasets with more than two samples were analyzed using one-way ANOVA followed by Tukey's post-hoc test.

Reporting summary. Further information on research design is available in the Nature Research Reporting Summary linked to this article.

Data availability

Sequence data that support the findings of this study have been deposited at <https://zenodo.org/record/3531884#XcQ7WIX7SUK>. All other data that support the findings of this study are included in Source Data file accompanying the manuscript or are available from the authors upon reasonable request.

Received: 20 March 2019; Accepted: 7 November 2019;

Published online: 05 December 2019

References

- Surmeier, D. J., Obeso, J. A. & Halliday, G. M. Selective neuronal vulnerability in Parkinson disease. *Nat. Rev. Neurosci.* **18**, 101–113 (2017).
- Chang, D. et al. A meta-analysis of genome-wide association studies identifies 17 new Parkinson's disease risk loci. *Nat. Genet.* **49**, 1511–1516 (2017).
- Pankratz, N. et al. Meta-analysis of Parkinson's disease: identification of a novel locus, RIT2. *Ann. Neurol.* **71**, 370–384 (2012).
- Li, J. Q., Tan, L. & Yu, J. T. The role of the LRRK2 gene in parkinsonism. *Mol. Neurodegener.* **9**, 47 (2014).
- Paisan-Ruiz, C. et al. Cloning of the gene containing mutations that cause PARK8-linked Parkinson's disease. *Neuron* **44**, 595–600 (2004).
- Monfrini, E. & Di Fonzo, A. Leucine-rich repeat kinase (LRRK2) genetics and Parkinson's Disease. *Adv. Neurobiol.* **14**, 3–30 (2017).
- Biskup, S. & West, A. B. Zeroing in on LRRK2-linked pathogenic mechanisms in Parkinson's disease. *Biochim Biophys. Acta* **1792**, 625–633 (2009).
- Zimprich, A. et al. Mutations in LRRK2 cause autosomal-dominant parkinsonism with pleomorphic pathology. *Neuron* **44**, 601–607 (2004).
- West, A. B. et al. Parkinson's disease-associated mutations in leucine-rich repeat kinase 2 augment kinase activity. *Proc. Natl Acad. Sci. USA* **102**, 16842–16847 (2005).
- Greggio, E. et al. Kinase activity is required for the toxic effects of mutant LRRK2/dardarin. *Neurobiol. Dis.* **23**, 329–341 (2006).
- Di Maio, R. et al. LRRK2 activation in idiopathic Parkinson's disease. *Sci. Transl. Med.* **10**, <https://doi.org/10.1126/scitranslmed.aar5429> (2018).
- Nguyen, M. & Krainc, D. LRRK2 phosphorylation of auxilin mediates synaptic defects in dopaminergic neurons from patients with Parkinson's disease. *Proc. Natl Acad. Sci. USA* **115**, 5576–5581 (2018).
- Manzoni, C. The LRRK2-macroautophagy axis and its relevance to Parkinson's disease. *Biochem Soc. Trans.* **45**, 155–162 (2017).
- Chen, Z. et al. LRRK2 interacts with ATM and regulates Mdm2-p53 cell proliferation axis in response to genotoxic stress. *Hum. Mol. Genet.* **26**, 4494–4505 (2017).
- Russo, I., Bubacco, L. & Greggio, E. LRRK2 and neuroinflammation: partners in crime in Parkinson's disease? *J. Neuroinflammation* **11**, 52 (2014).
- Wallings, R., Manzoni, C. & Bandopadhyay, R. Cellular processes associated with LRRK2 function and dysfunction. *FEBS J.* **282**, 2806–2826 (2015).
- Henderson, M. X., Peng, C., Trojanowski, J. Q. & Lee, V. M. Y. LRRK2 activity does not dramatically alter alpha-synuclein pathology in primary neurons. *Acta Neuropathol. Commun.* **6**, 45 (2018).
- Bezard, E., Yue, Z., Kirik, D. & Spillantini, M. G. Animal models of Parkinson's disease: limits and relevance to neuroprotection studies. *Mov. Disord.* **28**, 61–70 (2013).
- Burbulla, L. F. et al. Dopamine oxidation mediates mitochondrial and lysosomal dysfunction in Parkinson's disease. *Science* **357**, 1255–1261 (2017).
- Aharon-Peretz, J., Rosenbaum, H. & Gershoni-Baruch, R. Mutations in the glucocerebrosidase gene and Parkinson's disease in Ashkenazi Jews. *N. Engl. J. Med.* **351**, 1972–1977 (2004).
- O'Regan, G., deSouza, R. M., Balestrino, R. & Schapira, A. H. Glucocerebrosidase mutations in parkinson disease. *J. Parkinsons Dis.* **7**, 411–422 (2017).
- Spitz, M. et al. Association of LRRK2 and GBA mutations in a Brazilian family with Parkinson's disease. *Parkinsonism Relat. Disord.* **21**, 825–826 (2015).
- Duran, R. et al. The glucocerebrosidase E326K variant predisposes to Parkinson's disease, but does not cause Gaucher's disease. *Mov. Disord.* **28**, 232–236 (2013).
- Yahalom, G. et al. Carriers of both GBA and LRRK2 mutations, compared to carriers of either, in Parkinson's disease: Risk estimates and genotype-phenotype correlations. *Parkinsonism Relat. Disord.* **62**, 179–184, (2018).

25. Kriks, S. et al. Dopamine neurons derived from human ES cells efficiently engraft in animal models of Parkinson's disease. *Nature* **480**, 547–551 (2011).
26. Mazzulli, J. R., Zunke, F., Isacson, O., Studer, L. & Krainc, D. alpha-Synuclein-induced lysosomal dysfunction occurs through disruptions in protein trafficking in human midbrain synucleinopathy models. *Proc. Natl Acad. Sci. USA* **113**, 1931–1936 (2016).
27. Lorincz, M., Herzenberg, L. A., Diwu, Z., Barranger, J. A. & Kerr, W. G. Detection and isolation of gene-corrected cells in Gaucher disease via a fluorescence-activated cell sorter assay for lysosomal glucocerebrosidase activity. *Blood* **89**, 3412–3420 (1997).
28. Fell, M. J. et al. MLI-2, a potent, selective, and centrally active compound for exploring the therapeutic potential and safety of LRRK2 kinase inhibition. *J. Pharm. Exp. Ther.* **355**, 397–409 (2015).
29. Zheng, J. et al. Conversion of quinazoline modulators from inhibitors to activators of beta-glucocerebrosidase. *J. Med. Chem.* **62**, 1218–1230, (2019).
30. Sidransky, E. & Lopez, G. The link between the GBA gene and parkinsonism. *Lancet Neurol.* **11**, 986–998 (2012).
31. Steger, M. et al. Phosphoproteomics reveals that Parkinson's disease kinase LRRK2 regulates a subset of Rab GTPases. *Elife* **5**, <https://doi.org/10.7554/eLife.12813> (2016).
32. Eguchi, T. et al. LRRK2 and its substrate Rab GTPases are sequentially targeted onto stressed lysosomes and maintain their homeostasis. *Proc. Natl Acad. Sci. USA* **115**, E9115–E9124 (2018).
33. De Wit, T., Baekelandt, V. & Lobbstaal, E. LRRK2 Phosphorylation: behind the scenes. *Neuroscientist* **24**, 486–500 (2018).
34. Ysselstein, D., Shulman, J. M. & Krainc, D. Emerging links between pediatric lysosomal storage diseases and adult parkinsonism. *Mov. Disord.*, <https://doi.org/10.1002/mds.27631> (2019).
35. Alcalay, R. N. et al. Glucocerebrosidase activity in Parkinson's disease with and without GBA mutations. *Brain* **138**, 2648–2658 (2015).
36. Atashrazm, F. et al. Reduced glucocerebrosidase activity in monocytes from patients with Parkinson's disease. *Sci. Rep.* **8**, 15446 (2018).
37. Fedorow, H. et al. Neuromelanin in human dopamine neurons: comparison with peripheral melanins and relevance to Parkinson's disease. *Prog. Neurobiol.* **75**, 109–124 (2005).
38. Nguyen, A. P. & Moore, D. J. Understanding the GTPase activity of LRRK2: regulation, function, and neurotoxicity. *Adv. Neurobiol.* **14**, 71–88 (2017).
39. Boon, J. Y., Dusonchet, J., Trengrove, C. & Wolozin, B. Interaction of LRRK2 with kinase and GTPase signaling cascades. *Front Mol. Neurosci.* **7**, 64 (2014).
40. Takahashi, K. et al. Induction of pluripotent stem cells from adult human fibroblasts by defined factors. *Cell* **131**, 861–872 (2007).
41. Haeussler, M. et al. Evaluation of off-target and on-target scoring algorithms and integration into the guide RNA selection tool CRISPOR. *Genome Biol.* **17**, 148 (2016).
42. Deng, X. et al. Characterization of a selective inhibitor of the Parkinson's disease kinase LRRK2. *Nat. Chem. Biol.* **7**, 203–205 (2011).

Acknowledgements

We thank the Northwestern University Stem Cell Core Facility for the generation of the iPSC lines. Imaging work was performed at the Northwestern University

Center for Advanced Microscopy generously supported by CCSG P30 CA060553 awarded to the Robert H Lurie Comprehensive Cancer Center. D.Y. was supported by NIH grant T32NS041234, M.N. was supported by NIH grant 2T32AG020506–16, M.S. received a Heisenberg fellowship from the Deutsche Forschungsgemeinschaft (DFG) and D.K. was supported by NIH grants R01 NS076054, R37 NS096241, and a grant from the Michael J. Fox Foundation Parkinson's Research (D.K. and K.M.).

Author contributions

D.Y. and D.K. designed the overall study, analyzed data, wrote the manuscript, and edited the manuscript. D.Y., M.N., T.Y., and A.S. performed or assisted with experiments. M.S. and K.M. provided helpful advice on the study and edited the manuscript. All authors have read and approved the final manuscript.

Competing interests

D.K. is a scientific advisor for Preval Therapeutics and Intellia Therapeutics, as well as a venture partner at Orbimed. D.Y., M.N., T.Y., A.S., M.S., and K.M. declare no competing interests.

Additional information

Supplementary information is available for this paper at <https://doi.org/10.1038/s41467-019-13413-w>.

Correspondence and requests for materials should be addressed to D.K.

Peer review information *Nature Communications* thanks Huaibin Cai, Austen Milnerwood and the other, anonymous, reviewer(s) for their contribution to the peer review of this work.

Reprints and permission information is available at <http://www.nature.com/reprints>

Publisher's note Springer Nature remains neutral with regard to jurisdictional claims in published maps and institutional affiliations.



Open Access This article is licensed under a Creative Commons Attribution 4.0 International License, which permits use, sharing, adaptation, distribution and reproduction in any medium or format, as long as you give appropriate credit to the original author(s) and the source, provide a link to the Creative Commons license, and indicate if changes were made. The images or other third party material in this article are included in the article's Creative Commons license, unless indicated otherwise in a credit line to the material. If material is not included in the article's Creative Commons license and your intended use is not permitted by statutory regulation or exceeds the permitted use, you will need to obtain permission directly from the copyright holder. To view a copy of this license, visit <http://creativecommons.org/licenses/by/4.0/>.

© The Author(s) 2019